Establishment of human induced trophoblast stem-like cells from term villous cytotrophoblasts

Tao Bai[a], **Chian-Yu Peng**[a], **Ivy Aneas**[b], **Noboru Sakabe**[b], **Daniela F. Requena**[c], **Christine Billstrand**[b], **Marcelo Nobrega**[b], **Carole Ober**[b], **Mana Parast**[c], **John A. Kessler**[a,*]

[a] Department of Neurology, Northwestern University, Chicago, USA

[b] Department of Human Genetics, University of Chicago, Chicago, USA

[c] Department of Pathology and Sanford Consortium for Regenerative Medicine, University of California, San Diego, USA

Abstract

Human trophoblast stem cells (hTSC) can be isolated from first trimester placenta but not from term placenta. Here we demonstrate that villous cytotrophoblasts (vCTB) from term placenta can be reprogrammed into induced trophoblastic stem-like cells (iTSC) by introducing sets of transcription factors. The iTSCs express TSC markers such as GATA3, TEAD4 and ELF5, and are multipotent, validated by their differentiation into both extravillous trophoblasts (EVT) and syncytiotrophoblasts (STB) *in vitro* and *in vivo*. The iTSC can be passaged indefinitely *in vitro* without slowing of growth. The transcriptome profile of these cells closely resembles the profile of hTSC isolated from first trimester placentae but different from the term placental vCTB from which they originated. The ability to reprogram cells from term placenta into iTSC will allow study of early gestation events which impact placental function later in gestation, including preeclampsia and spontaneous preterm birth.

Keywords

Placenta; Trophoblast; Stem cell; Reprogramming; Differentiation

1. Introduction

Mouse trophoblast stem cells (mTSC) were isolated more than 20 years ago from outgrowths of either the blastocyst polar trophectoderm (TE) or extraembryonic ectoderm (ExE) of post implantation embryos (Tanaka, Kunath et al., 1998). However, isolation of well-characterized human TSC (hTSC) from outgrowths of either blastocysts or more mature cytotrophoblasts from first trimester chorionic villi was only recently reported (Okae et al., 2018). These primary hTSC had a transcriptome profile most similar to those of first trimester cytotrophoblast (CTB), were capable of self-renewal, and could be differentiated into both syncytiotrophoblasts (STB) and extravillous trophoblasts (EVT) *in vitro.* However, attempts to isolate and culture hTSC in their undifferentiated state from term placenta have been unsuccessful (Okae et al., 2018). More recently, 3D trophoblast organoids expressing markers of trophoblast identity and stemness were also derived by two groups, but again, only from first trimester chorionic villi (Haider et al., 2018; Turco et al., 2018). The requirement for first trimester human tissues poses ethical and practical issues that limit studies with hTSC and trophoblast organoids, including the inability to conduct studies with tissues with known pregnancy outcomes.

Here we used a strategy similar to iPSC reprogramming to generate human "induced" trophoblast stem-like cells (iTSC) from term vCTB. We transduced sets of five or six transcription factors into vCTB isolated from term placental cores and generated cell lines that proliferate and self-renew, have epithelial morphology, express TSC-associated markers, and are capable of differentiation into STB and EVT. The transcriptome profile of these cells closely conforms to the profile of hTSC derived from first trimester chorionic villi. This protocol for reprogramming term vCTB into iTSC will facilitate study of abnormal processes in early gestation which are the basis for placental dysfunction in diseases of later pregnancy.

2. Materials and methods

2.1. Tissue collection and isolation of villous cytotrophoblasts (vCTB)

Term placentae (Gestation week 38–40) were obtained upon delivery at Prentice Women's Hospital and University of Chicago Hospital. Utilization of tissues was approved by the Institutional Review Board (IRB) and required written informed consent. CTB were isolated from fresh placental tissues as described previously (Kliman et al., 1986). Briefly, two pieces of 3 by 3 cm placental tissue were dissected and rinsed with sterile 0.9% saline. Tissue surrounding chorionic villous vessels were scraped and chopped into 1–2 mm pieces with forceps, followed by three sequential digestions in enzymatic cocktail containing 3.4% Dispase (Corning #354235), 0.2% Trypsin (Sigma # T9935), and 0.05% Dnase (Roche #104159). Dissociated cells were filtered through a 100 μm cell strainer, with cell debris and other undesired cell populations removed following Percoll density gradient (5–70%) centrifugation. Recovered villous CTBs were washed and frozen for later use.

2.2. Derivation of iTSCs

Retroviral constructs expressing human GATA3, TFAP2C, TEAD4, CDX2, ELF5, ETS2 were used for reprogramming vCTB to iTSC. Human ORF for these transcription factors were purchased from GE Darmachon or GeneCopoeia (see supplemental Table 2 for details), subcloned into retroviral vector pMXs, and confirmed by sequencing. Individual retroviral vectors were transfected into the packaging cell line PLAT-A (Cell Biolabs). Viral supernatant was collected at 48, 72 and 120 h and concentrated by Retro-X Concentrator (Clontech). For reprogramming, vCTB were seeded at a density of 300,000–500,000 per well in ESC-qualified Matrigel-coated 6-well plates (Corning #354277). 24 h later, pooled retrovirus containing 5 or 6 factors was added to individual wells according to experimental design. The viruses were removed the next day and cells were fed with DMEM media containing 10%FBS. 48 h after viral transduction, cells were switched to modified TSC media (Advanced DMEM/F-12 supplemented with 1X B27/N2 (Thermo Fisher), 0.05% BSA (Sigma A8412), 0.15 mM 1-thioglycerol (Sigma-Aldrich), 1% KSR, 2 mM CHIR99021, 0.5 mM A83–01, 1 mM SB43154 (Tocris Biotechne), 0.8 mM VPA, 5 mM Y27632, 100 ng/ml FGF2 (Thermo Fisher), 50 ng/ml EGF (Millipore), 50 ng/ml HGF (Stem Cell Technology) and 20 ng/ml Noggin (R&D System). Reprogrammed cells were cultured at 37 °C and 5% CO2. The culture media was replenished every other day. The cells were passaged by TrypLE (Thermo Fisher) every 3–7 days to a new Matrigel-coated 6-well plate at a 1:3–1:6 split ratio. Twelve cell lines were generated from four reprogramming experiments with different combination of transcription factors, using cells from four individual placentae. Cells between passages 5–15 were used for characterization. iTSC were compared to an hTSC cell line (line #1049), derived from first trimester (6-week gestational age) placental tissues, in the Parast lab at UC San Diego and previously characterized (Morey et al., in press).

2.3. Differentiation of iTSC

EVT differentiation was performed through the modification of a protocol described previously (Okae et al., 2018). iTSC were seeded at a density of 0.75×10^5 per well in Col-IV-coated ibidi μ-dishes in EVT differentiation medium (EVTM: advanced DMEM/F12, 0.1 mM 2-mercaptoethanol (Gibco 31350), 0.3% BSA, 1% ITS-X supplement (Gibco 51500–056), 100 ng/ml NRG1 (Cell Signaling 5218SC), 7.5 μM A83–01, 4% knockout serum replacement (ThermoFisher 10828010), and 2% Matrigel. After 3 days, the medium was changed to EVTM, 0.5% Matrigel without NRG1 for a further 3–4 days. Then, immunostaining of HLA-G was performed on the differentiated EVT in ibidi μ-dishes.

STB differentiation was induced using a modified protocol described previously (Okae et al., 2018). The cells were seeded in a 6-well plate or coverslips pre-coated with 2.5 μg/ml Col IV at a density of 10^5 cells per well or 2.5×10^4 per coverslip, and cultured in 2 mL or 0.5 mL of STB medium (Advanced DMEM/F12 supplemented with 1XB27/N2, 0.05% BSA, 2.5 mM Y27632, 2 mM forskolin, and 4% KSR). Multi-nucleated morphology of syncytiotrophoblast was observed on day 3–7 of differentiation. Immunostaining for hCG was performed on day 3 as cells began to lift from culture plates during day 4–7 of differentiation.

2.4. Immunostaining

Cells plated on Matrigel-coated coverslips were fixed in 4% paraformaldehyde (PFA) for 15 min, permealized with 0.25% Triton-X for 10 min, blocked with 10% goat serum/0.1% Tween-20/PBS at RT for 1 h. Cells were incubated with primary antibodies diluted in 1% BSA/PBST at 4 °C overnight, washed with 0.1% Tween-20/PBS for 3 times, then incubated with secondary antibodies and DAPI for 1 h, washed with PBST, then mounted. Images were captured with a Zeiss Axiovert microscope and Axiovision imaging software SE64 V4.9.1. Primary antibodies used in this study were GATA3 (Abcam #ab199428), TFAP2C (Abcam #ab218107), TEAD4 (Abcam #ab155244), p63 (Abcam #ab124762), CDX2 (Cell Signaling Technology #12306), ELF5 (Santa Cruz Technology # SC-376373), HLA-G (clone 4H84 Abcam #ab25455), hCG (Invitrogen #MA1–19063) CK7 (DAKO #M7018), hPL (Abcam #ab25138), and Ki67 (Abcam #ab15580).

2.5. Invasion assay

1×10^5 iTSC were seeded on Transwell polycarbonate inserts (6.5 mm with 8-μm pores; Costar Corp.) that were coated with 10 μl of undiluted Matrigel (Ilic, Kapidzic et al., 2008). The EVT differentiation medium used in upper and bottom chambers were EVTM containing NRG1 and 2% Matrigel for 3 days and EVTM containing 0.5% Matrigel but without NRG1 for 3–4 days. iTSC cultured in the TSC medium was used as a control. After 7 days, the cultures were 4% PFA for 15 min and immunostained for CK7 and HLA-G. Non-invading cells on top of the transwell were removed using a cotton swab, and the membrane cut out by a scalpel, mounted on a slide with the underside of the membrane facing upward under a glass coverslip and imaged by confocal microscopy. The presence or the absence of cells with bipolar morphology expressing CK7 or HLA-G was used as a measure of cell invasion.

2.6. Quantitative real-time PCR analysis

Total RNA was prepared using the RNeasy mini Kit and RNase-free DNase (QIAGEN). First-strand cDNA was synthesized from total RNA using high capacity RNA-to-cDNA kit (Applied Biosystems), and real-time PCR reaction was done with SYBR Green master mix and TaqMan™ Universal Master Mix II, with UNG (Thermo Fisher). Differential gene expression between experimental groups was determined using the Ct method with GAPDH as the internal control from at least three independent experiments and presented as fold difference between groups. All primers used are listed in supplemental Table 1.

2.7. Modified teratoma assay

Use of mice for these assays was approved by the Insitutional Animal Care and Use Committee (IACUC) at UC San Diego. iTSCs were grown to 90% confluence in modified TSC medium (as described above) and dissociated with TrypLE. 3×10^7 iTSCs were resuspended in 0.3 mL of a 1:2 mixture of Matrigel and TSC medium, and subcutaneously injected into the flank and hindleg of 8–12-week-old male NOD-SCID mice (JAX Stock No: 005557). Tumor growths were collected 10 days after injection. The tumors were fixed in 10% neutral-buffered formalin overnight at 4 °C, embedded in paraffin, and sectioned at 5 μm. Sections were stained with hematoxylin-eosin (H&E), or processed for

immunostaining with antibodies against EGFR1 (1:15, Roche, cat#790–4347), TP63 (1:150, Biocare Medical, cat#ACI3066A), HLA-G (1:6000, Abcam, cat#ab52455) and hCG (1:300, Abcam, cat#ab9582), and detected using an HRP-based reaction with the tyramide Alexa Fluor fluorescence system (ThermoFisher) on a Ventana Discovery Ultra (Roche). Prior to immunostaining, antigen retrieval was performed by incubation with CC1 (Tris-EDTA; pH 8.5) for 40 min at 95 °C. For Dual immunofluorescence, the first primary was applied (hCG or TP63) to the tissue sections and detected using the UltraMap donkey anti-mouse (760–4313) secondary antibody followed by fluorescent-labeling with TSA-Alexa 594 (ThermoFisher, cat#B40957). The antibody was fully denatured, inactivated, and removed from the tissue by treatment in CC2 (pH 6.5; Ventana) for 20 min at 95 °C. Next, the antibody targeting EGFR was applied to the slides and detected with the OmniMap donkey anti-rabbit secondary (760–4311) antibody followed by reaction with TSA-Alexa 488 (ThermoFisher, cat# B40953). Slides were rinsed and coverslipped with Prolong gold antifade with DAPI (Thermofisher).

2.8. RNA sequencing

Total RNA was extracted from approximately 1 million cells from passage 10–15 iTSC cultures using RNeasy mini kit (Qiagen), according to manufacturer's instructions. RNA quality and concentration were assessed using a Bioanalyzer 2100 (Agilent technology). 1 ug of total RNA was used for library preparation using NEBNext Ultra II Directional RNA Library Prep Kit for Illumina (NEB), and RNA sequencing was performed on the Illumina HiSeq 4000 at the University of Chicago Genomics Core Facility.

2.9. Differential expression analysis

Read counts per gene and TPMs from RNA sequencing were calculated with Salmon (Patro et al., 2017) version 0.12.0. Estimated counts were used in exploratory analysis (transformed with DESeq2′s rlog function for principal component analysis) and in DESeq2 (Love et al., 2014) version 1.24.0 to identify differentially expressed genes (adjusted p-value   0.05 and absolute fold-change of   1.2). Svaseq (Leek, 2014) identified 6 surrogate variables that were used in the DESeq2 analysis. The heatmap shows Z-scores of mean TPMs per gene.

3. Results

3.1. Reprogramming term placenta villous cytotrophoblasts into expandable iTSCs

To generate human iTSC lines (Fig. 1A), villous cytotrophoblasts (vCTBs) from term placental cores were isolated and cultured as a monolayer according to published protocols (Longtine, Chen et al., 2012). Purity of the culture was assessed 24hrs after plating by immunocytochemical staining of epithelial marker cytokeratin 7 (Ck7) and stromal cell marker Vimentin (Vim), along with cell cycle marker Ki67. Ck7 expression was detected in greater than 93.2 ± 1.1% of viable cells, with Ki67 expression only detected in 5.8 ± 1.1% of Ck7$^+$ cells (Fig. 1C). Vim is detected in only 3.8 ± 0.6% of the cells with no overlapping Ki67 expression. These findings suggest that the starting culture is highly enriched in cells of the cytotrophoblast lineage. At 24hrs post plating (Fig. 1C'), cells were transduced with or without retroviruses expressing various combinations of transcription factors (GATA3, TFAP2C, CDX2, TEAD4, ELF5 and ETS2) (Fig. 1B), and then cultured in

modified TSC media containing a mixture of growth factors and small molecule inhibitors. The growth factors and small molecule inhibitors chosen for use in TSC media were based on previous reports on mouse and human TSC (Ohinata and Tsukiyama 2014, Okae et al., 2018). No formation of proliferative colonies or significant changes in cell morphology were observed in vCTB cultured in the TSC media without the reprogramming factors (data not shown), suggesting that the TSC media alone is not sufficient to induce changes in vCTB cell fate. Except for ETS2 for self-renewal, each individual transcription factor was removed from the transcription factor pool to examine which combination of these factors might generate the maximal iTSC population. Fourteen to 21 days after the initial transduction, small populations of epithelial-like cells emerged within differentiated STBs in wells transduced with either all six factors or five factors without GATA3 or TEAD4 (Fig. 1D). On day 28–35, the epithelial-like cells were harvested and passaged onto new Matrigel-coated plates. They initially grew slowly, but soon required passaging every 3–5 days at a ratio of 1:6–1:12. These cell lines all showed similar growth and morphology. The cells were expanded for more than 5 months (passage 20) without any slowing of growth or change in morphology (Fig. 1E). Qualitative comparison of colony forming ability among the experimental conditions suggested the most effective combination of reprogramming factors was TFAP2C, TEAD4, CDX2, ELF5, and ETS2 (Well 2 in Fig. 1B). Due to its proliferative efficiency, we were able to quickly expand progenies from this line and will mainly focus our subsequent analyses from this iTSC line (hereafter referred as 5F–G3). Cell lines were also established from colonies formed in cultured transduced with 6 factors and 5 factors without TEAD4 (5F-T4) for additional characterizations.

To determine whether the established cell lines retain expression of reprogramming transgenes, we performed real-time quantitative-PCR analyses with primers specifically targeting transgenic transcripts using mRNA isolated from 5F-G3 and 5F-T4 iTSC lines. We found that transgene specific transcripts did not significantly differ between 5F-G3 lines and the control vCTB that lack the transgene, suggesting that transgenic expression of the reprogramming factors is not maintained in the 5F-G3 lines after passaging (Supplementary Fig. 2A). In contrast, transgene specific transcripts for TFAP2c, ETS2, and CDX2 were strongly detected in the 5F-T4 lines, indicating genomic integration of the viral vectors (Supplementary Fig. 2B). These findings further reinforced our decision to focus on the 5F-G3 lines.

3.2.   iTSC express known markers of human trophoblastic stem cells

To investigate whether the reprogramming factors contribute to changes in vCTB molecular properties, we next examined protein expression of TSC-associated markers that were not a part of our reprogramming cocktail by Immunocytochemistry (ICC) after 5 passages. We found that cells generated from the 5F-G3 line, which lack the GATA3 transgene, showed positive staining of GATA3 (Fig. 2A), indicating that they had acquired this TSC-associated marker. Similarly, TSC-associated protein p63 (Fig. 2F) (Li et al., 2014) and other genes expressed by cytotrophoblasts and proliferative epithelial cells (ITGA6, CDH1, and CK7 – Fig. 2E, G, H), also were detected in the 5F-G3 line by ICC. CDX2, a part of the 5-factor cocktail, was not detected in the 5F-G3 line (Fig. 2I), confirming that the transgene is either silenced or lost during passaging. Unlike the starting vCTB, majority of the 5F-T3 cells

express the cell cycle marker Ki67, indicating their proliferative nature (Fig. 2J). Taken together, these findings suggest the 5F-G3 lines express many of the TSC enriched proteins and maintain proliferative capacity over many passages.

3.3. iTSC cells differentiate into STB and EVT

Human TSC derived from first trimester placentas, as well as TSC derived from hESCs, can differentiate into both STB and EVT (Okae et al., 2018, Dong et al., 2020, Cinkornpumin et al., 2020). To determine whether the iTSC lines are functionally similar to hTSC, we assessed the differentiation potential of iTSC lines into syncytiotrophoblasts (STB) and extravillous trophoblasts (EVT). After 3–4 days of culture of the iTSC in the STB differentiation medium modified from Okae et al., multinucleated cells were formed that expressed the STB markers human chorionic gonadotropin (hCG); hCG was detected in $86.4 \pm 4.5\%$ of DAPI+ cells in STB media, but not detected in cells cultured in TSC media (Fig. 2K, 2K'). Ability to differentiate into the EVT lineage was assessed by adapting an EVT differentiation protocol for the iTSC. Cells with elongated morphology express the EVT marker HLA-G constituted $97.2 \pm 2.5\%$ of DAPI + cells after 7 days in EVT media, while cells grown in TSC media failed to express HLA-G after 7 days (Fig. 2L, 2L'). Similar to the iTSC 5F-G3 line, iTSCs derived from 6 factor transductions were also able to differentiate into STB and EVT (Supplementary Fig. 3). A functional feature of EVT is their ability to penetrate membranes mimicking their invasive behavior *in vivo* into maternal decidua. Therefore, iTSCs were grown on Matrigel-coated Transwell inserts in EVT differentiation media to assess their invasive capacity, with those cultured in TSC media as comparisons (Fig. 2M). CK7 and HLA-G expressing cells with bipolar morphology were only detected on the opposing side of the plated membrane surface in cultures with EVT differentiation media, and not in control cultures grown in TSC media (Fig. 2M–2N'). Taken together, these findings suggest iTSC respond to differentiation signals and generate progenies that are morphologically, molecularly, and functionally homologous to EVT.

3.4. Transcriptome profiling of human iTSC

To determine whether the iTSC have a gene expression pattern similar to the pattern in human TSC established from 1st trimester villi, and different from vCTB from term placenta, we performed RNA-Seq analysis on iTSC, hTSC and vCTB. Principal component analysis (PCA) plotting PC1 against PC2 revealed that the iTSC closely grouped with the hTSC but were widely distinct from vCTB, from which the iTSC were reprogrammed (Fig. 3A). 3D plotting showed some variance among the groups of iTSC and hTSC on the PC3 axis (Fig. 3A). Examination of known hTSC marker gene expression revealed similar expression patterns between iTSC and hTSC, which were distinct from those in term vCTB (Fig. 3B and C). For example, CTNNB1 (β-catenin) and ITGA6 are similarly highly expressed in iTSC and hTSC by transcript detected (Fig. 3C), but relatively low in comparison to first trimester CTB (Fig. 3B). On the other hand, endogenous ELF5 transcripts were marginally detected in iTSC and hTSC (Fig. 3C), but are significantly higher in comparison to vCTB by both RNAseq and qRT-PCR (Fig. 3B and 3D). Furthermore, higher levels of TSC marker TEAD4 mRNA was detected in iTSC and hTSC by both RNAseq and qRT-PCR analyses when compared to vCTB (Fig. 3B and 3D). CDX2, EOMES and ESRRB, required for mouse TSC maintenance and self-renewal, were absent

in hTSC and iTSC, accounting for the species discrepancy in trophoblast specification and development.

3.5. Human iTSC differentiate into STB and EVT in mouse transplantation model

Ability to form teratomas is a key assay used in the murine stem cell field to demonstrate lineage differentiation. To investigate the *in vivo* differentiation potential of iTSC, both iTSC and hTSC were subcutaneously injected into the flank and hindleg of non-obese diabetic (NOD)-severe combined immunodeficiency (SCID) mice. After 10 days, lesions were noted in mice injected with either cell line. H&E staining revealed a subcutaneous tumor with a necrotic center, surrounded by a rim of mononuclear and multinucleated cells, some with rather enlarged nuclei and irregular chromatin (Fig. 4A). Both the hTSC and iTSC tumors showed a combination of EGFR/p63 double-positive mononuclear, CTB-like cells, hCG$^+$ multinucleated STB-like cells, and HLA-G$^+$ mononuclear EVT-like cells (Fig. 4/B). Interestingly, the latter were more numerous in iTSC-derived tumors, compared to hTSC-derived tumors (Fig. 4B, right panels). These findings suggest iTSC are capable of differentiating into STB and EVT without exogenous signals in this *in vivo* transplantation model.

4. Discussion

Human embryonic stem cell lines derived from blastocysts became available in 1998, and opened entirely new areas of research in human embryology (Thomson et al., 1998). However, progress was limited by ethical issues surrounding the need for human embryos to create such lines. The discovery in 2006 that somatic cells could be reprogrammed into iPSC revolutionized the field and greatly accelerated study of both normal human development and the pathophysiology of human disease (Takahashi and Yamanaka, 2006, Takahashi et al., 2007). Study of the human trophoblastic lineage and of diseases of pregnancy benefited from the ability to reprogram iPSC and ESC to cells with the characteristics of the trophoblast lineage, but the transcriptome signature of these cells is not fully equivalent to the transcriptome of primary trophoblast (Horii et al., 2020). Isolation of well-characterized human TSC (hTSC) from outgrowths of either blastocysts or more mature cytotrophoblasts from first trimester villi was only reported in 2018 (Okae et al., 2018), and more recently techniques were developed for creating TSC from naïve ESC/iPSC (Dong et al., 2020, Cinkornpumin et al., 2020, Io et al., 2021, Guo et al., 2021). However, the need for blastocysts or first trimester placental tissue to generate hTSC is an impediment, and issues related to loss of imprinting may preclude the use of naïve hPSCs in modeling placental disease (Cinkornpumin et al., 2020). By contrast, placental tissue is abundantly available at term, can be obtained without biopsy or invasive procedures, and is accompanied by the pregnancy history and outcome. This prompted us to develop techniques for reprogramming vCTB to iTSC.

We found that non-integrating viral expression of TFAP2C, TEAD4, CDX2, ELF5, and ETS2 transcription factors efficiently generated TSC-like cells. The cells have a morphology similar to previously reported cultured hTSC obtained from first trimester tissue (Okae et al., 2018), and they had a transcriptome profile almost identical to hTSC. The iTSC and

hTSC largely overlapped in PC1 and PC2 analysis. The cells were able to generate STB and EVT and formed trophoblastic tumors in a modified teratoma assay (Okae et al., 2018). The iTSC proliferate rapidly but have shown no detectable variability during the 20 passages that have been tested thus far. Thus, this protocol should provide the field with large numbers of iTSCs from pregnancies with different outcomes.

In addition to the difference in the gestational age of starting cells, one key difference our protocol and the published TSC generation method reported by Okae et al is the substrate on which cells were plated during culture. The substrate used in the Okae protocol is Collagen IV, a common component of the basement membranes, on which vCTB sit and grow *in vivo* (Oefner et al., 2015). On the other hand, Matrigel is widely used for culturing human pluripotent stem cells for its biomimetic properties but is not molecularly well defined. Importantly, Matrigel is primarily constituted of Collagen and Laminin, which are ligands for integrin receptors that play important roles in both cell fate and stemness of multiple stem cell types. It is possible that the complexity of ECM substrates in Matrigel facilitate the reprogramming or maintenance of iTSC in our protocol. However, testing more defined substrates in future studies will expand the potential of iTSC for human uses. Although the transcriptome of the iTSC and hTSC almost completely overlapped, some differences were noted. Inhibitor of DNA binding 2 (ID2) which is expressed in proliferative CTB and cell column trophoblasts, was expressed in iTSC lines at higher levels than in hTSC, perhaps reflecting its role in the rapid proliferation of the lines (Janatpour et al., 2000, Soncin et al., 2018). Another key transcription factor heart and neural crest derivatives expressed 1 (HAND1), which is expressed in human TE but absent from first trimester cytotrophoblast (Knöfler et al., 1998; Soncin et al., 2018), was more variable in the lines generated compared to hTSC. Both RNAseq and qPCR data also revealed iTSC endogenously express higher levels of ELF5 and TEAD4, both of which have been associated with TSC self-renewal (Latos et al., 2015, Saha et al., 2020). These findings lend further support to the stem-like nature of the reprogrammed cells.

Although we did not observe viral vector integration in several reprogrammed cell lines, the possibility of retroviral integration exists and limits current iteration of the protocol in clinical or therapeutic applications. This shortcoming can be addressed in future experiments by expressing reprogramming factors using non-integrating Sendai viruses. Another potential improvement of the protocol is to further reduce the number of necessary reprogramming factors, which may raise the efficiency of transduction and reprogramming. Finally, given the recent finding of extensive mutagenesis and mosaicism in term placental tissues (Coorens et al., 2021), some caution is warranted in using these cells for generation of iTSC. Nevertheless, it is possible that this inherent feature is in fact also part of disease pathogenesis, and as such, the use of CTB from these tissues for iTSC generation would allow for capture of both genetic and epigenetic bases of trophoblast-based disorders of placentation.

In addition to facilitating further study of the human trophoblast lineage, the availability of large numbers of easily produced iTSC should be useful for drug screening. Pharmaceutical manufacturers almost never test new drugs in pregnant women, and most drugs thus are not labeled for use during pregnancy. Good screens for potential toxicity might help to

obviate this problem. Organoid models of the human endometrium have been developed (Turco et al., 2018; Chu Cheung et al., 2021), and ultimately co-culture models of iTSC with endometrial organoids would be most useful for this purpose.

Supplementary Material

Refer to Web version on PubMed Central for supplementary material.

Acknowledgements

References

Chu Cheung V, Peng CY, Marinic M, Sakabe NJ, Aneas I, Lynch VJ, Ober C, Nobrega MA, Kessler JA, 2021. Pluripotent cell cell-derived endometrial stromal fibroblasts in a cyclic, hormone-responsive, coculture model of human decidua. Cell Rep. 35(7):109138. [PubMed: 34010658]

Cinkornpumin JK, Kwon SY, Guo Y, Hossain I, Sirois J, Russett CS, Tseng H-W, Okae H, Arima T, Duchaine TF, Liu W, Pastor WA, 2020. Naive human embryonic stem cells can give rise to cells with a trophoblast-like transcriptome and methylome. Stem Cell Rep. 15 (1), 198–213.

Coorens THH, Oliver TRW, Sanghvi R, Sovio U, Cook E, Vento-Tormo R, Haniffa M, Young MD, Rahbari R, Sebire N, Campbell PJ, Charnock-Jones DS, Smith GCS, Behjati S, 2021. Inherent mosaicism and extensive mutation of human placentas. Nature 592 (7852), 80–85. [PubMed: 33692543]

Dong C, Beltcheva M, Gontarz P, Zhang B, Popli P, Fischer LA, Khan SA, Park KM, Yoon EJ, Xing X, Kommagani R, Wang T, Solnica-Krezel L, Theunissen TW, 2020. Derivation of trophoblast stem cells from naïve human pluripotent stem cells. Elife. 12 (9), e52504.

Guo G.e., Stirparo GG, Strawbridge SE, Spindlow D, Yang J, Clarke J, Dattani A, Yanagida A, Li MA, Myers S, Özel BN, Nichols J, Smith A, 2021. Human naive epiblast cells possess unrestricted lineage potential. Cell Stem Cell 28 (6), 1040–1056.e6. [PubMed: 33831366]

Haider S, Meinhardt G, Saleh L, Kunihs V, Gamperl M, Kaindl U, Ellinger A, Burkard TR, Fiala C, Pollheimer J, Mendjan S, Latos PA, Knöfler M, 2018. Self-renewing trophoblast organoids recapitulate the developmental program of the early human placenta. Stem Cell Rep. 11 (2), 537–551.

Horii M, Touma O, Bui T, Parast MM, 2020. Modeling human trophoblast, the placental epithelium at the maternal fetal interface. Reproduction 160 (1), R1–R11, 10.1530/REP-19-0428. [PubMed: 32485667]

Ilic D, Kapidzic M, Genbacev O (2008). "Isolation of human placental fibroblasts." Curr Protoc Stem Cell Biol Chapter 1: Unit 1C 6.

Io S, Kabata M, Iemura Y, Semi K, Morone N, Minagawa A, Wang B.o., Okamoto I, Nakamura T, Kojima Y, Iwatani C, Tsuchiya H, Kaswandy B, Kondoh E, Kaneko S, Woltjen K, Saitou M, Yamamoto T, Mandai M, Takashima Y, 2021. Capturing human trophoblast development with naive pluripotent stem cells in vitro. Cell Stem Cell 28 (6), 1023–1039.e13. [PubMed: 33831365]

Janatpour MJ, McMaster MT, Genbacev O, Zhou Y, Dong J, Cross JC, Israel MA, Fisher SJ, 2000. Id-2 regulates critical aspects of human cytotrophoblast differentiation, invasion and migration. Development 127 (3), 549–558. [PubMed: 10631176]

Kliman HJ, Nestler JE, Sermasi E, Sanger JM, Strauss JF 3rd, 1986. Purification, characterization, and in vitro differentiation of cytotrophoblasts from human term placentae. Endocrinology 118(4): 1567–1582. [PubMed: 3512258]

Knöfler M, Meinhardt G, Vasicek R, Husslein P, Egarter C, 1998. Molecular cloning of the human Hand1 gene/cDNA and its tissue-restricted expression in cytotrophoblastic cells and heart. Gene 224 (1–2), 77–86. [PubMed: 9931445]

Latos PA, Sienerth AR, Murray A, Senner CE, Masanaga M, Ikawa M, Oxley D, Burge S, Cox BJ, Hemberger M, 2015. Elf5-centered transcription factor hub controls trophoblast stem cell self-renewal and differentiation through stoichiometry-sensitive shift in target gene network. Genes Dev. 29 (23), 2435–2448. [PubMed: 26584622]

Leek JT, 2014. svaseq: removing batch effects and other unwanted noise from sequencing data. Nucleic Acids Res. 42 (21).

Li Y, Moretto-Zita M, Leon-Garcia S, Parast MM, 2014. p63 inhibits extravillous trophoblast migration and maintains cells in a cytotrophoblast stem cell-like state. Am. J. Pathol. 184 (12), 3332–3343. [PubMed: 25307348]

Love MI, Huber W, Ander S, 2014. Moderated estimation of fold change and dispersion for RNA-seq data with DESeq2. Genome Biol. 15, 550. [PubMed: 25516281]

Morey R, Farah O, Kallol S, Requena Gibert D, Meads M, Moretto-Zita M, Soncin F, Laurent LC, Parast MM, Transcriptomic drivers of differentiation, maturation, and polyploidy in human extravillous trophoblast. Front. Cell Develop. Biol., in press.

Oefner CM, Sharkey A, Gardner L, Critchley H, Oyen M, Moffett A, 2015. Collagen type IV at the fetal-maternal interface. Placenta 36 (1), 59–68. [PubMed: 25465704]

Ohinata Y, Tsukiyama T, 2014. Establishment of trophoblast stem cells under defined culture conditions in mice. PLoS ONE 9 (9), e107308. [PubMed: 25203285]

Okae H, Toh H, Sato T, Hiura H, Takahashi S, Shirane K, Kabayama Y, Suyama M, Sasaki H, Arima T.l., 2018. Derivation of human trophoblast stem cells. Cell Stem Cell 22 (1), 50–63. [PubMed: 29249463]

Patro R, Duggal G, Love MI, Irizarry RA, Kingsford C, 2017. Salmon provides fast and bias-aware quantification of transcript expression. Nat. Methods 14 (4), 417–419. [PubMed: 28263959]

Saha B, Ganguly A, Home P, Bhattacharya B, Ray S, Ghosh A, Rumi MAK, Marsh C, French VA, Gunewardena S, Paul S, 2020. TEAD4 ensures postimplantation development by promoting trophoblast self-renewal: an implication in early human pregnancy loss. Proc. Natl. Acad. Sci. U.S.A. 117 (30), 17864–17875. [PubMed: 32669432]

Soncin F, Khater M, To C, Pizzo D, Farah O, Wakeland A, Arul Nambi Rajan K, Nelson KK, Chang CW, Moretto-Zita M, Natale DR, Laurent LC, Parast MM, 2018. Comparative analysis of mouse and human placentae across gestation reveals species-specific regulators of placental development. Development 145 (2).

Takahashi K, Yamanaka S, 2006. Induction of pluripotent stem cells from mouse embryonic and adult fibroblast cultures by defined factors. Cell 126 (4), 663–676. [PubMed: 16904174]

Takahashi K, Tanabe K, Ohnuki M, Narita M, Ichisaka T, Tomoda K, Yamanaka S, 2007. Induction of pluripotent stem cells from adult human fibroblasts by defined factors. Cell 131 (5), 861–872. [PubMed: 18035408]

Thomson JA, Itskovitz-Eldor J, Shapiro SS, Waknitz MA, Swiergiel JJ, Marshal V.S.l., Jones JM, 1998. Embryonic stem cell lines derived from human blastocysts. Science 282 (5391), 1145–1147. [PubMed: 9804556]

Turco MY, Gardner L, Kay RG, Hamilton RS, Prater M, Hollinshead MS, McWhinnie A, Esposito L, Fernando R, Skelton H, Reimann F, Gribble FM, Sharkey A, Marsh SGE, O'Rahilly S, Hemberger M, Burton GJ, Moffett A, 2018. Trophoblast organoids as a model for maternal-fetal interactions during human placentation. Nature 564 (7735), 263–267. [PubMed: 30487605]
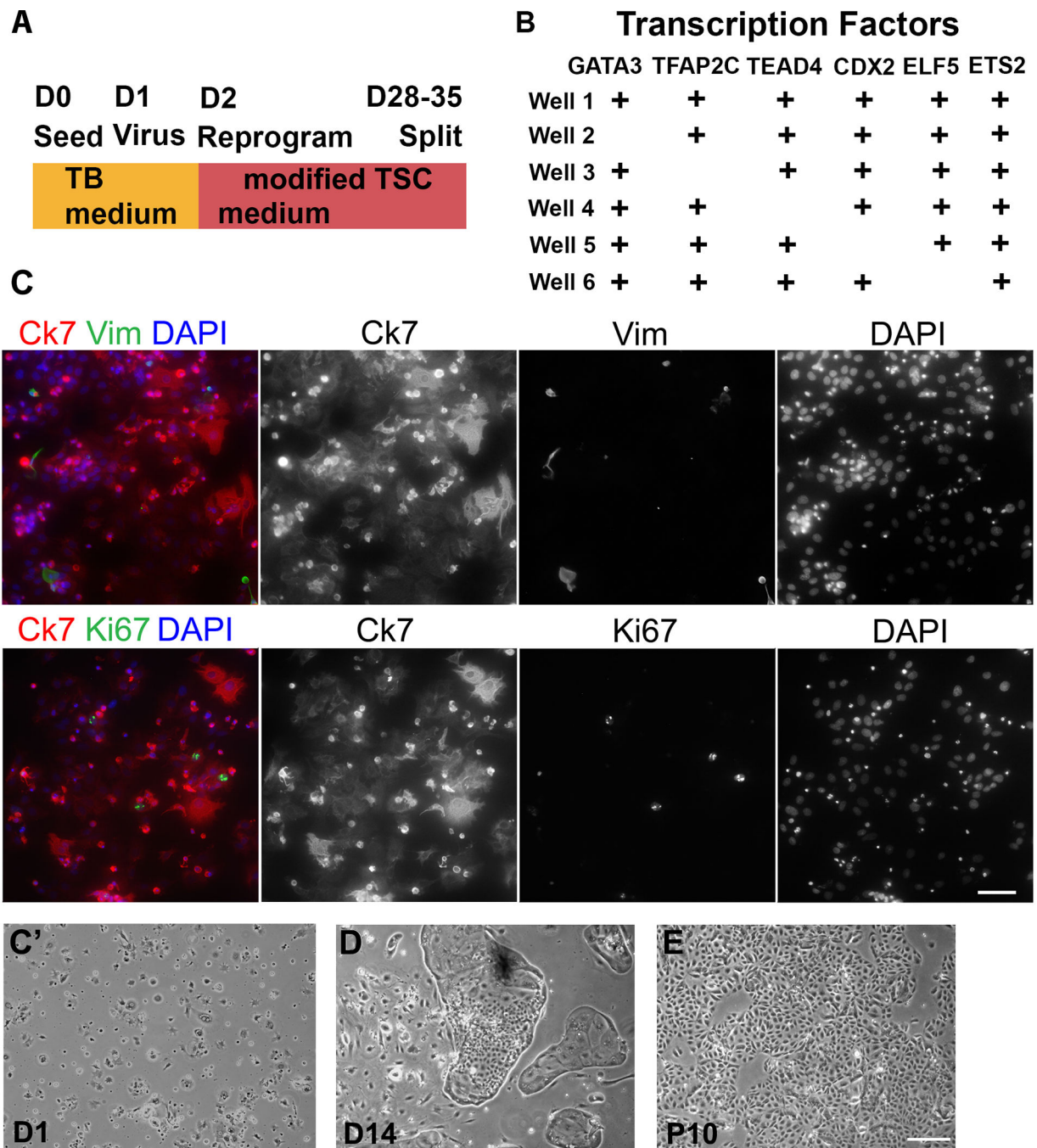
A

D0	D1	D2	D28-35
Seed	Virus	Reprogram	Split

TB medium | modified TSC medium

B

Transcription Factors

	GATA3	TFAP2C	TEAD4	CDX2	ELF5	ETS2
Well 1	+	+	+	+	+	+
Well 2		+	+	+	+	+
Well 3	+		+	+	+	+
Well 4	+	+		+	+	+
Well 5	+	+	+		+	+
Well 6	+	+	+	+		+

C

Ck7 Vim DAPI | Ck7 | Vim | DAPI

Ck7 Ki67 DAPI | Ck7 | Ki67 | DAPI

C' D1 **D** D14 **E** P10

Fig. 1.

Reprogramming term placental villous cytotrophoblasts to iTSC. (A) Schematic representation of protocols to reprogram term vCTB to iTSC. (B) Mixtures of 5–6 transcription factors (TFs) were used to induce reprogramming of term vCTB. Isolated vCTB from term placental cores were transduced under the indicated combinations of TFs for 1 day. The transduced cells were switched to reprogramming medium 24 h after removal of virus mixtures. The signs of + indicate included transcription factors. (C) Immunofluorescent images of vCTB prior to viral transduction stained with epithelial

marker cytokeratin 7 (CK7), stromal marker Vimentin (Vim), and cell cycle marker Ki67. (C'-E) Phase-contrast images of cells from well 2 (5 factors minus GATA3) at day 1 (D1), day 14 (D14), and after 10 passages (P10) showing an epithelial-like colony emerging within the differentiated STB sheet around day 14–21 (D), and remain morphologically similar and proliferative at passage 10 (E). Scale bar, C = 100 μm; D-F = 500 μm.
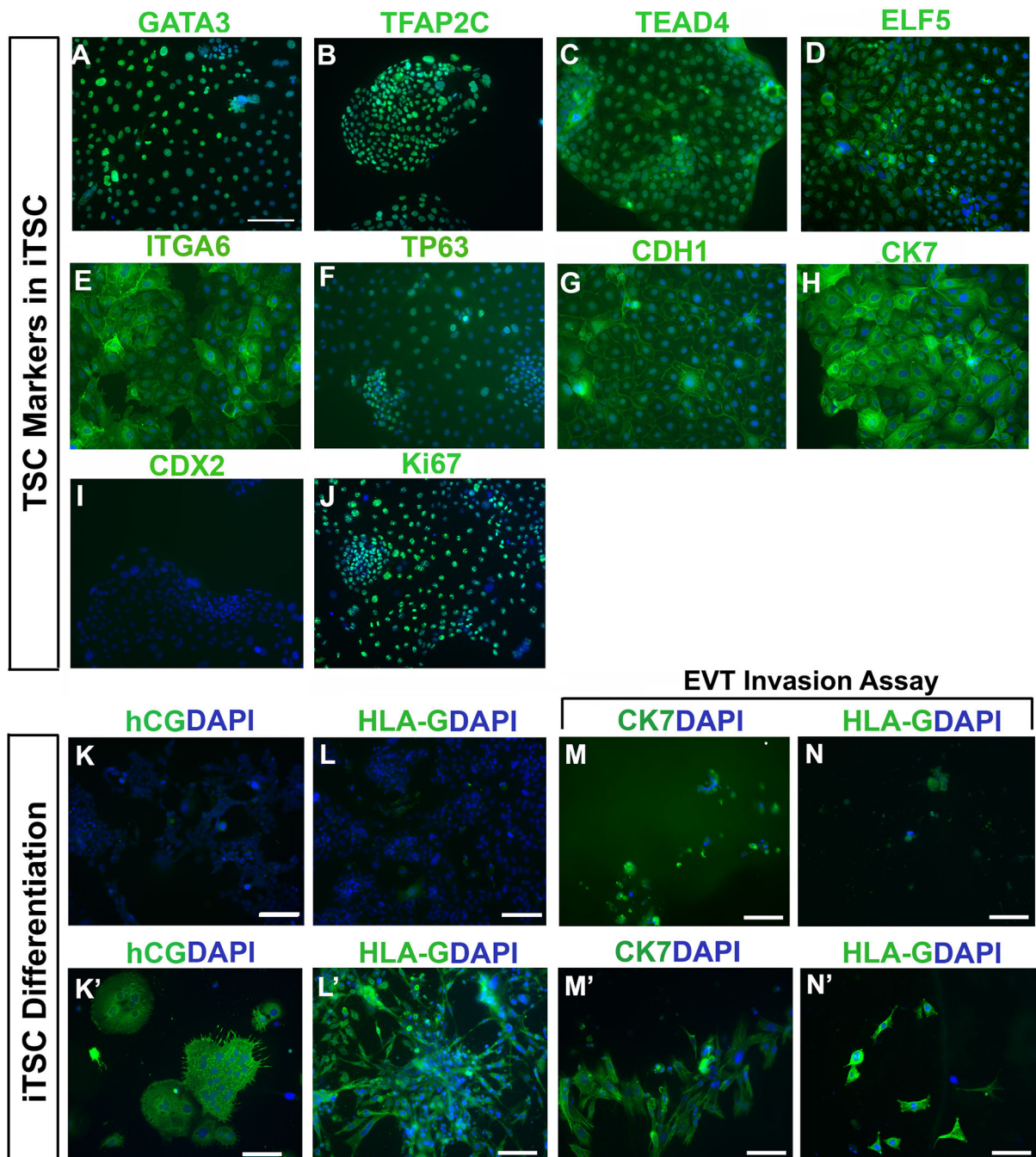
Fig. 2.
Detection of hTSC markers in iTSC and STB and EVT markers after iTSC differentiation.
(A-J) Immunostaining for TSC markers GATA3, TFAP2C, TEAD4, ELF5, ITGA6, TP63,
CDH1, CK7 and Ki67 (Green) in 5F-G3 iTSC at passage 10–15. Nuclei were stained with
DAPI (Blue). Similar results were obtained with three independent cell lines generated
using the six factors (sup Fig. 1). (K, K') Immunostaining of STB marker hCG (green)
in iTSC cultured in TSC medium (K) or STB differentiation medium (K') at 3 days *in
vitro* demonstrating the capacity of iTSC to generate of multinucleated syncytiotrophoblasts

under appropriate differentiation conditions. Similar results were obtained with two independent cell lines. (L, L') Immunostaining of HLA-G (green) in iTSC cultured in TSC medium (L) or EVT differentiation medium (L') at 7 days *in vitro* demonstrating the capacity of iTSC to generate HLA-G$^+$ cells with bipolar morphology under appropriate differentiation conditions. Similar results were obtained with two independent cell lines. (M-N') Representative images of CK7 (M') and HLA-G (N') expressing cells detected on the bottom surface of the Transwell membrane after iTSC cultured in TSC medium (M, N) or EVT medium (M', N') on the top surface of Transwell membrane for 7 days. Only iTSC cells in EVT differentiation medium penetrated Transwells membrane. scale bar = 100 μm.
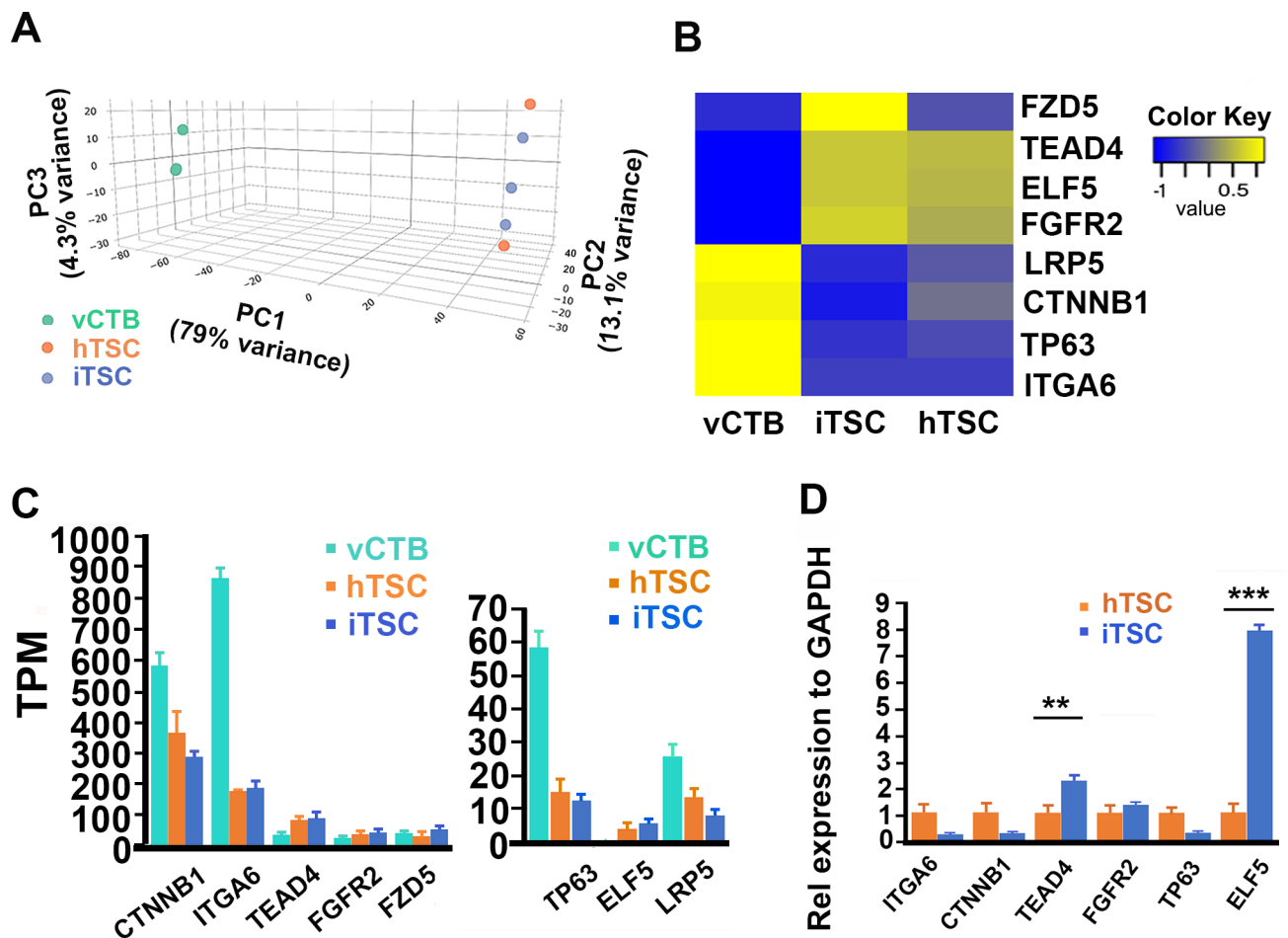
Fig. 3.
RNA-Sequencing revealed transcriptome level similarities between iTSC and hTSC. (A) Principle component analysis of hTSC, iTSC and untreated term cytotrophoblasts, iTSC and hTSC aligned closely on the PC1 and PC2 axes but showed variability on the PC3 axis. All data points were collected with three technical triplicates. (B) Expression comparisons of proliferative cytotrophoblast-related genes between vCTB, hTSC and iTSC revealed iTSCs show similar expression profiles with hTSC and significant differences from vCTB. (C) Expression levels of proliferative cytotrophoblast-related genes in primary and reprogrammed iTSC cells. Data are presented as mean + SD. n = 3 technical triplicates. (D) Quantitative real-time PCR analysis of proliferative cytotrophoblast-related gene expression in vCTB (n = 3) and iTSC (n = 3). The transcript level of TEAD4 was higher (2.16 fold increase, p < 0.01) in iTSC than in vCTB. Similarly, ELF5 expression in elevated in iTSC compared to vCTB (7.6 fold increase, p < 0.001. The data were normalized to GAPDH expression and represented as fold change relative to vCTB. ** p < 0.01; ***p < 0.001.
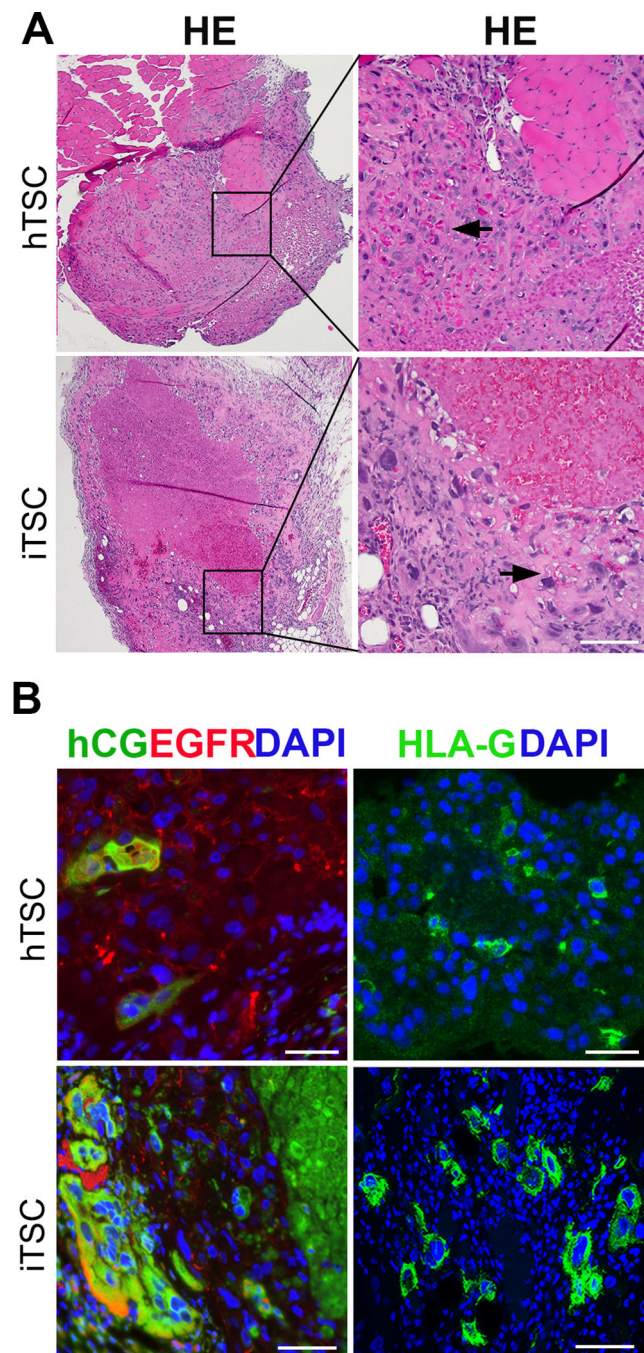
Fig. 4.
Modified teratoma assays demonstrate differentiation of iTSC into STB and EVT lineages
in vivo. (A) Hematoxylin-eosin (HE) staining in hTSC and iTSC-derived lesion images
at 4X magnification (right panel) with 10X magnification view of the lesion boarder
(right panel). Some STB-like trophoblast cells contained blood-filled lacunae (arrows). (B)
Immunofluorescence images of hTSC and iTSC-derived lesions. Differentiation into STB
and EVT in the lesion was demonstrated by immunostaining of EGFR1 (red) and hCG

(green) for STB and for HLA-G (green) for EVT with nuclei stained with DAPI. Scale bar, A = 100 μm, B = 50 μm.